Electronic Supplementary Material (ESI) for Physical Chemistry Chemical Physics.
This journal is © the Owner Societies 2018

Supporting information

Ethanol Synthesis from Syngas over Cu(Pd)-doped Fe(100) : A Systematic Theoretical Investigation

Wei Wang [1], Ye Wang *[,2], and Gui-Chang Wang*[,1,3]

([1]College of Chemistry, Key Laboratory of Advanced Energy Materials Chemistry (Ministry of Education) and Collaborative Innovation Center of Chemical Science and Engineering(Tianjin), Nankai University, Tianjin 300071, P. R. China; [2] State Key Laboratory of Physical Chemistry of Solid Surfaces, National Engineering Laboratory for Green Chemical Productions of Alcohols, Ethers and Esters, College of Chemistry and Chemical Engineering, Xiamen University, Xiamen 361005, China; [3] State Key Laboratory of Coal Conversion, Institute of Coal Chemistry, Chinese Academy of Sciences, Taiyuan, 030001, P. R. China)

*Corresponding author: Gui-Chang Wang. E-mail: wangguichang@nankai.edu.cn

Ye Wang. E-mail: wangye@xmu.edu.cn

Telephone: +86-22-23503824 (O) Fax: +86-22-23502458

Contents:

Figure S1. Optimized adsorption structures of the reaction intermediates involved in the syngas reaction on Fe_9/Fe(100)

Figure S2. Optimized adsorption structures of the reaction intermediates involved in the syngas reaction on Cu_9/Fe(100)

Figure. S3. Optimized adsorption structures of the reaction intermediates involved in the syngas reaction on Fe_3Pd_6/Fe(100).

Figure S4. Optimized configurations for the main TSs involved in the reactions on Fe_9/Fe(100)

Figure S5. Optimized configurations for the main TSs involved in the reactions on Cu_9/Fe(100)

Figure S6. Optimized configurations for the main TSs involved in the reactions on Fe_3Pd_6/Fe(100)..

Figure S7. The projected DOS onto d-band of (a) Fe_9/Fe(100), (b) Fe_3Cu_6/Fe(100) and (c) Cu_9/Fe(100) surfaces

Figure S8. The DRC distribution of the elementary steps toward (a) CH_4, (b) CH_3OH and (c) CH_3CH_2OH formation on the Fe_9/Fe(100) surfaces. Note: +/− in brackets refers to the positive or negative values of DRC, corresponding to promotion or inhibition effects on the rate.

Figure S9. The DRC distribution of the elementary steps toward (a) CH_4, (b) CH_3OH and (c) CH_3CH_2OH formation on the Cu_9/Fe(100) surfaces. Note: +/− in brackets refers to the positive or negative values of DRC, corresponding to promotion or inhibition effects on the rate.

Figure S10. The DRC distribution of the elementary steps toward (a) CH_4, (b) CH_3OH and (c) CH_3CH_2OH formation on the Fe_3Pd_6/Fe(100) surfaces. Note: +/− in brackets refers to the positive or negative values of DRC, corresponding to promotion or inhibition effects on the rate.

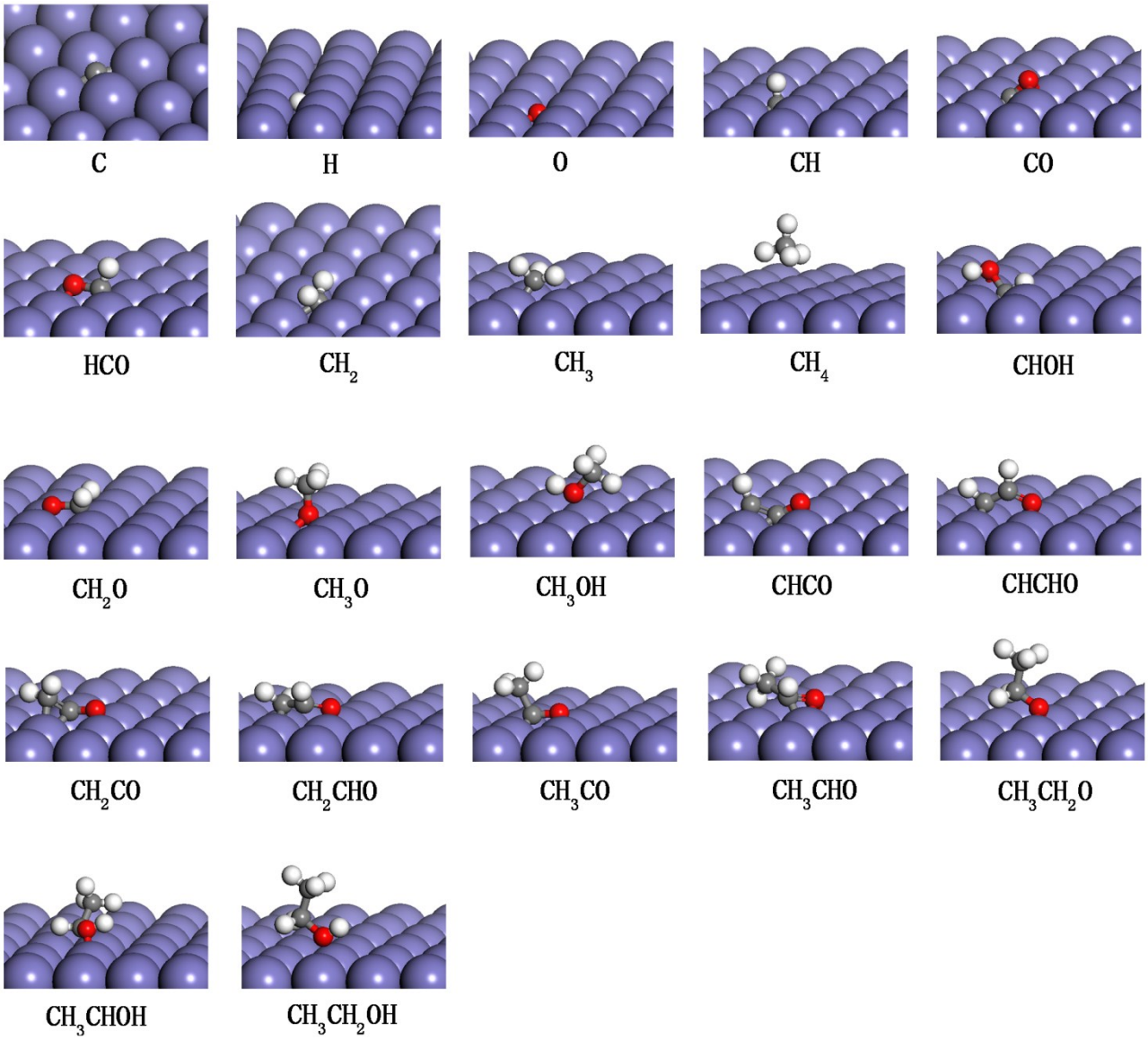

Figure S1. Optimized adsorption structures of the reaction intermediates involved in the syngas reaction on Fe_9/Fe(100)

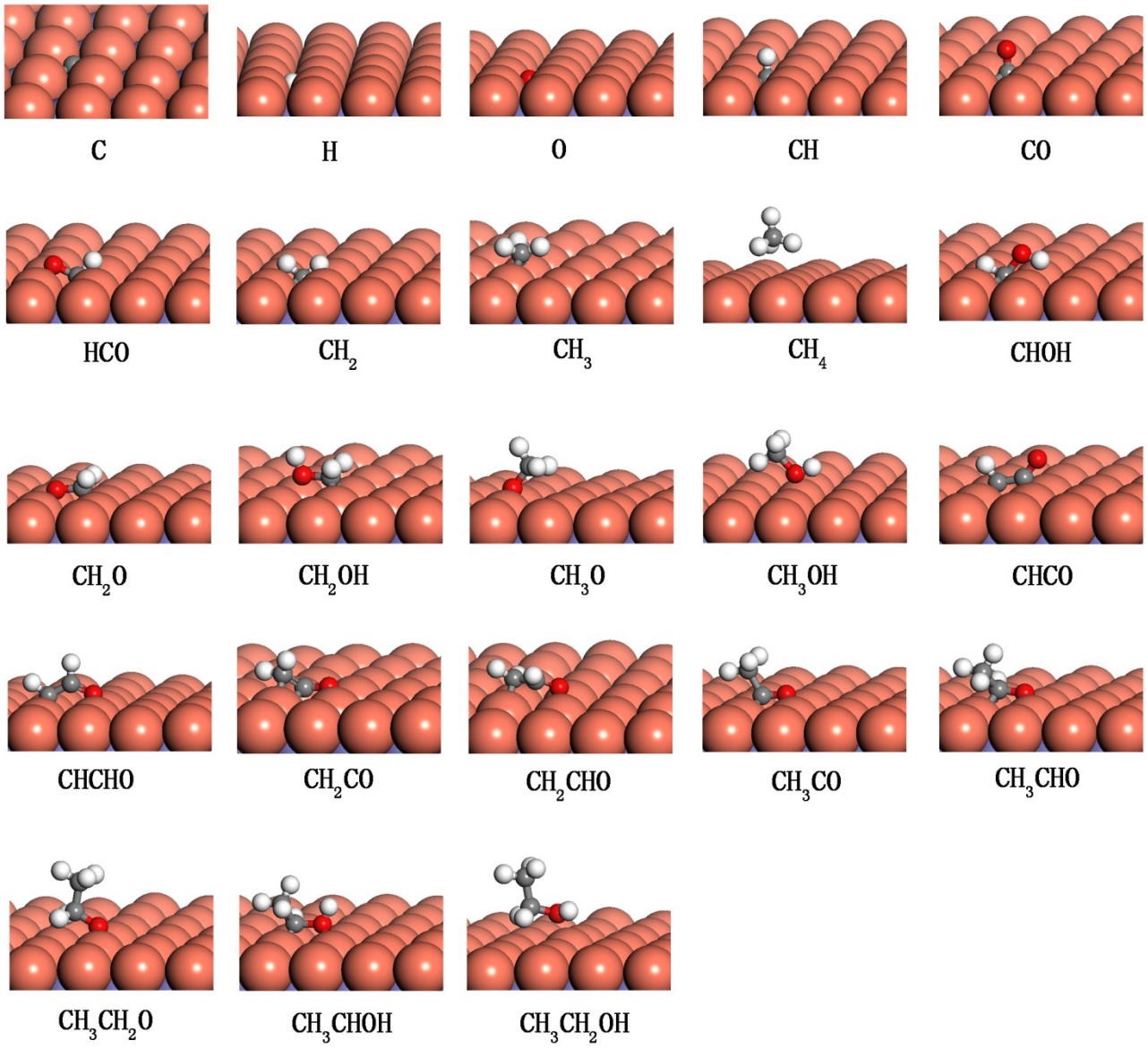

Figure S2. Optimized adsorption structures of the reaction intermediates involved in the syngas reaction on Cu_9/Fe(100)

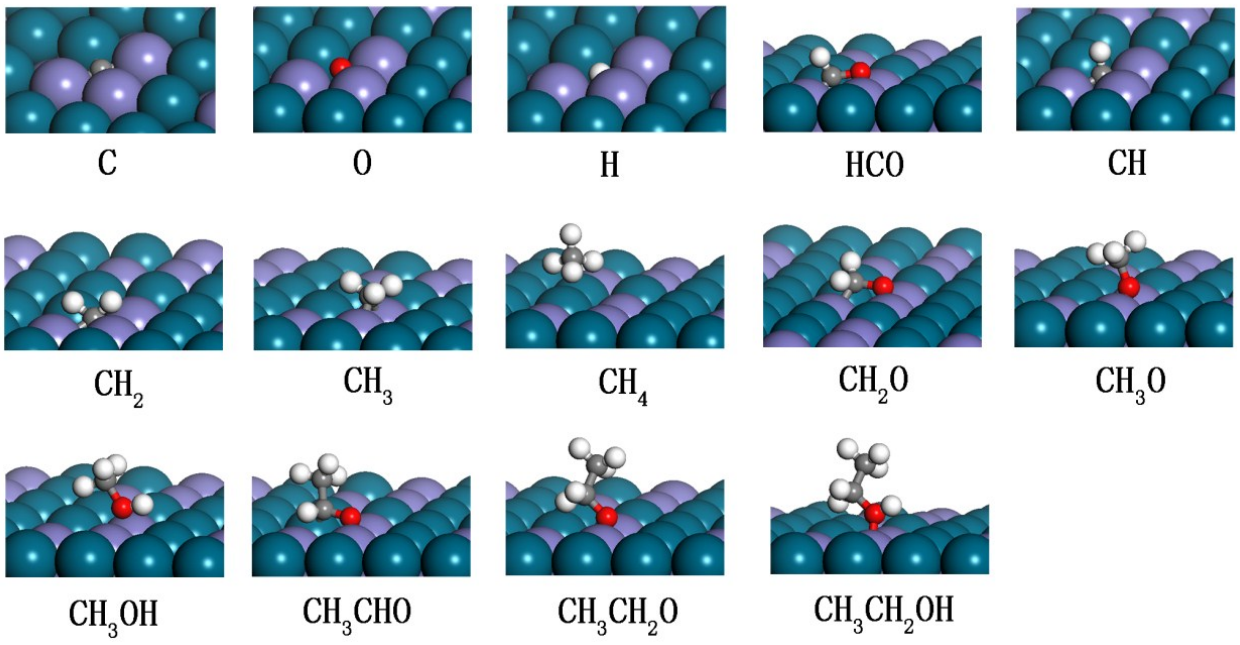

Figure S3. Optimized adsorption structures of the reaction intermediates involved in the syngas reaction on Fe_3Pd_6/Fe(100)

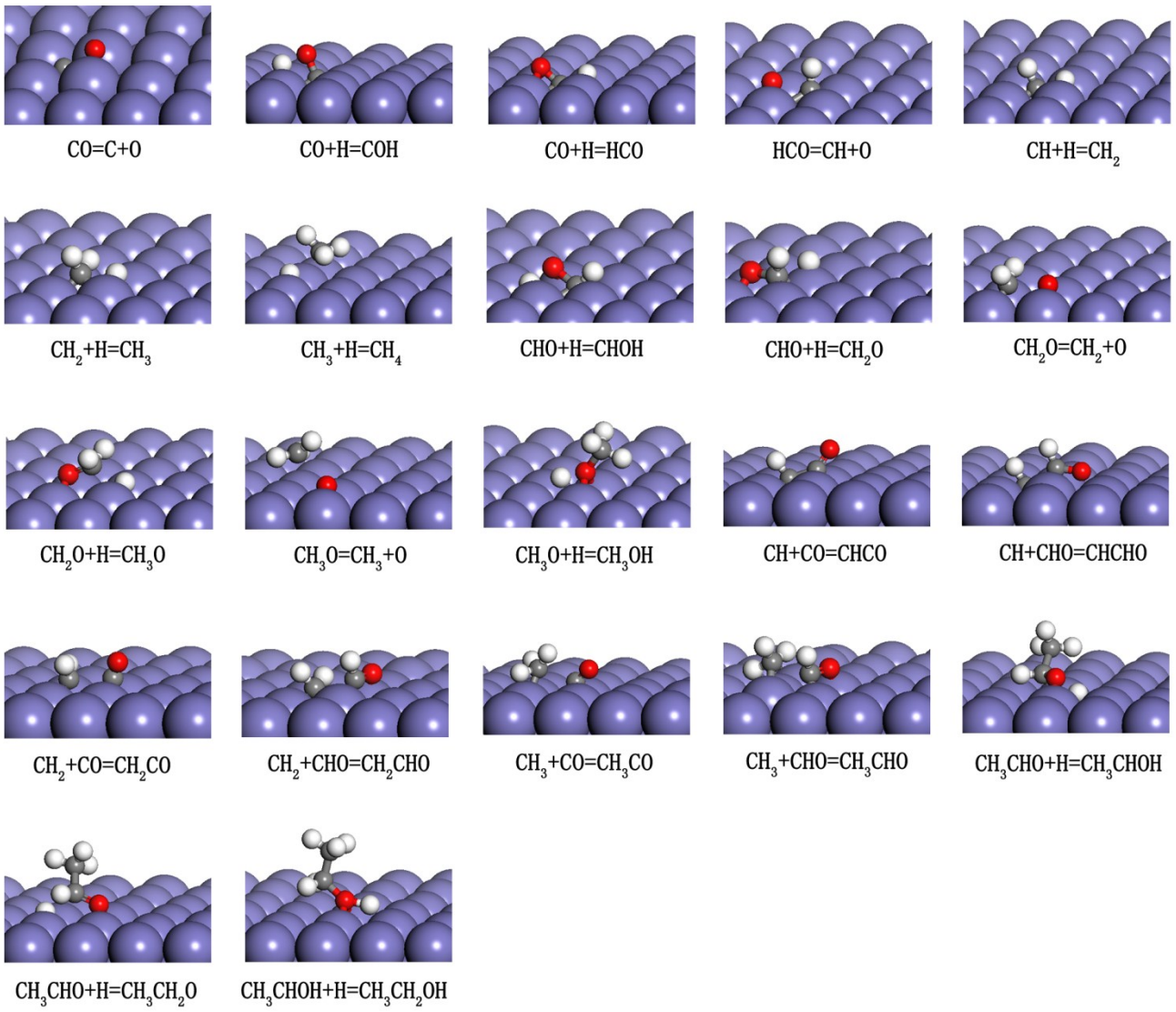

Figure. S4 Optimized configurations for the main TSs involved in the reactions on Fe_9/Fe(100).

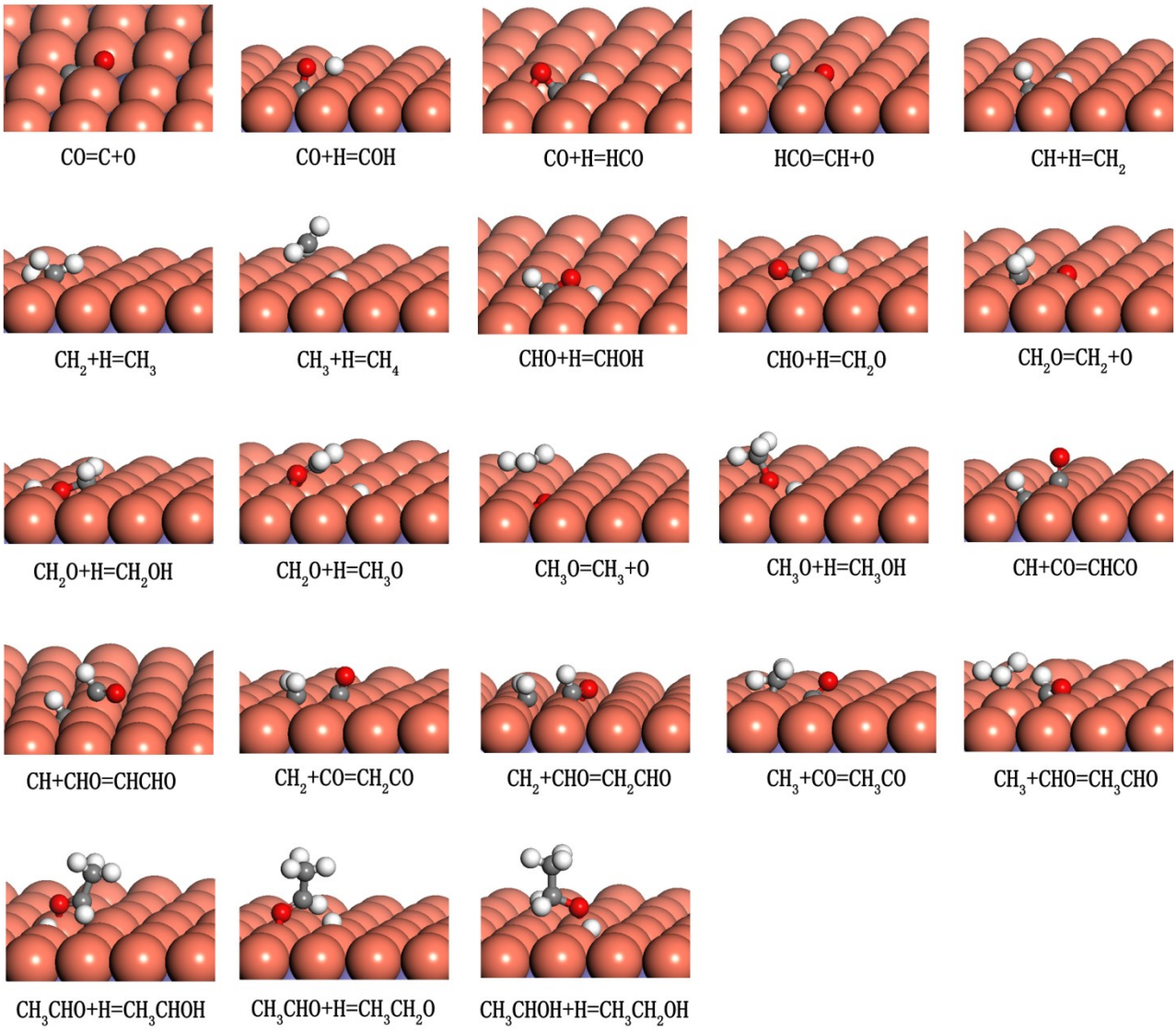

Figure. S5 Optimized configurations for the main TSs involved in the reactions on Cu_9/Fe(100).

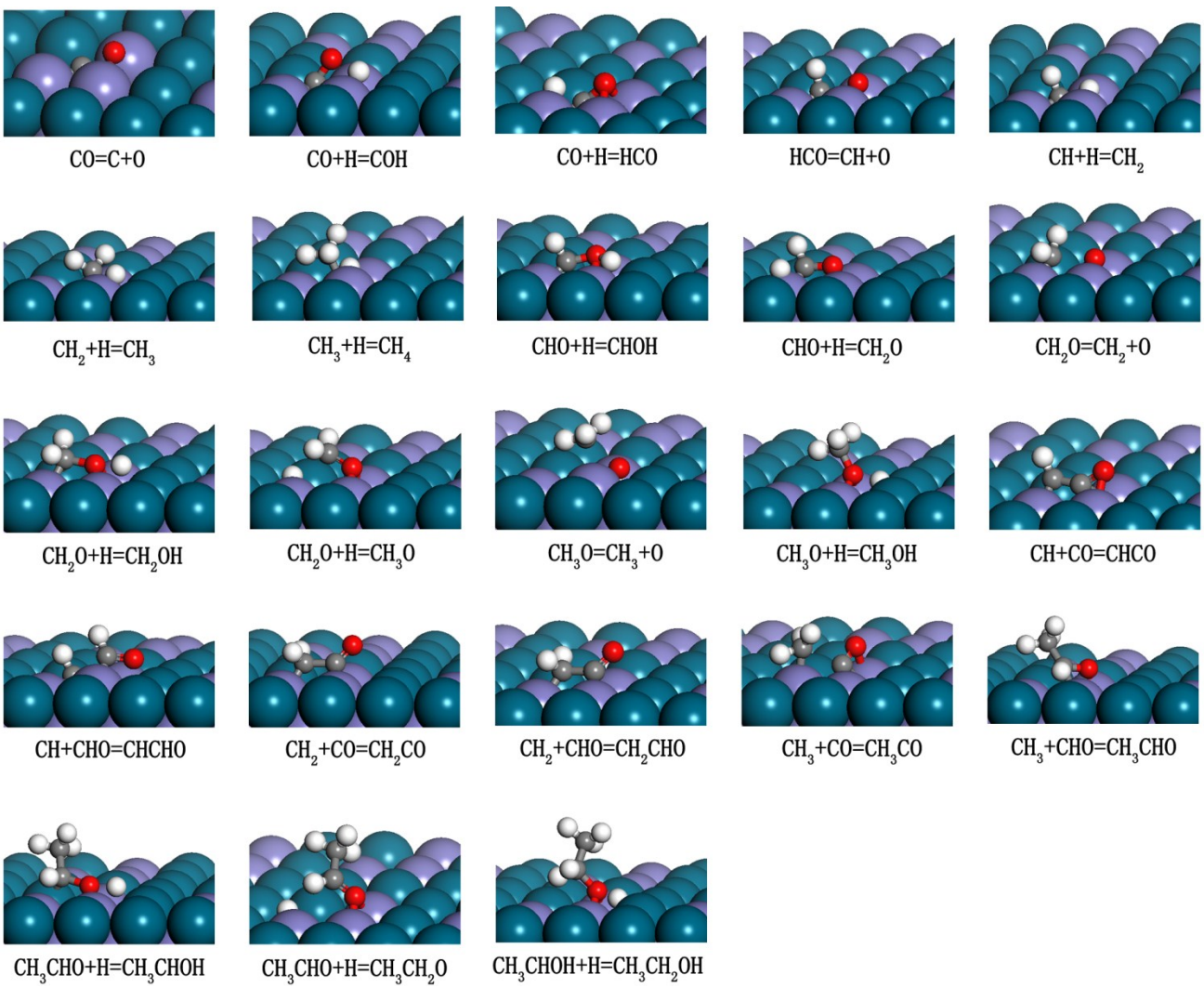

Figure. S6 Optimized configurations for the main TSs involved in the reactions on Fe_3Pd_6/Fe(100).

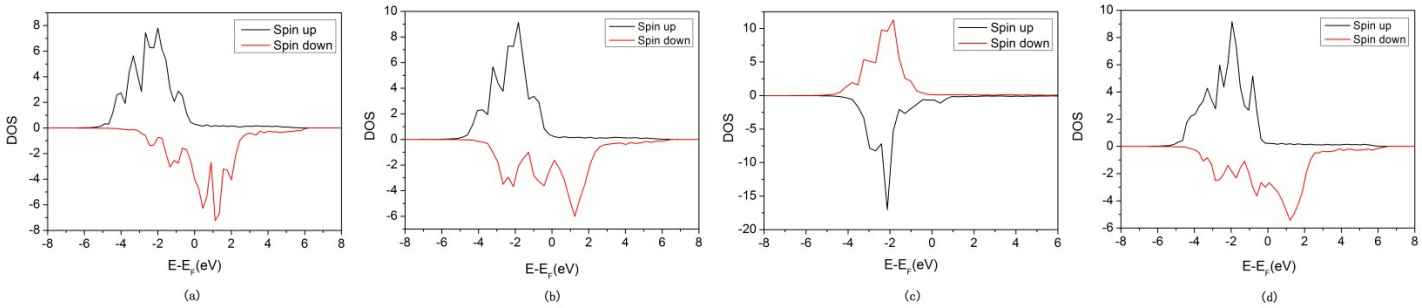

Figure S7. The projected DOS onto d-band of (a) Fe_9/Fe(100), (b) Fe_3Cu_6/Fe(100), (c) Cu_9/Fe(100), and (d) Fe_3Pd_6/Fe(100) surfaces.

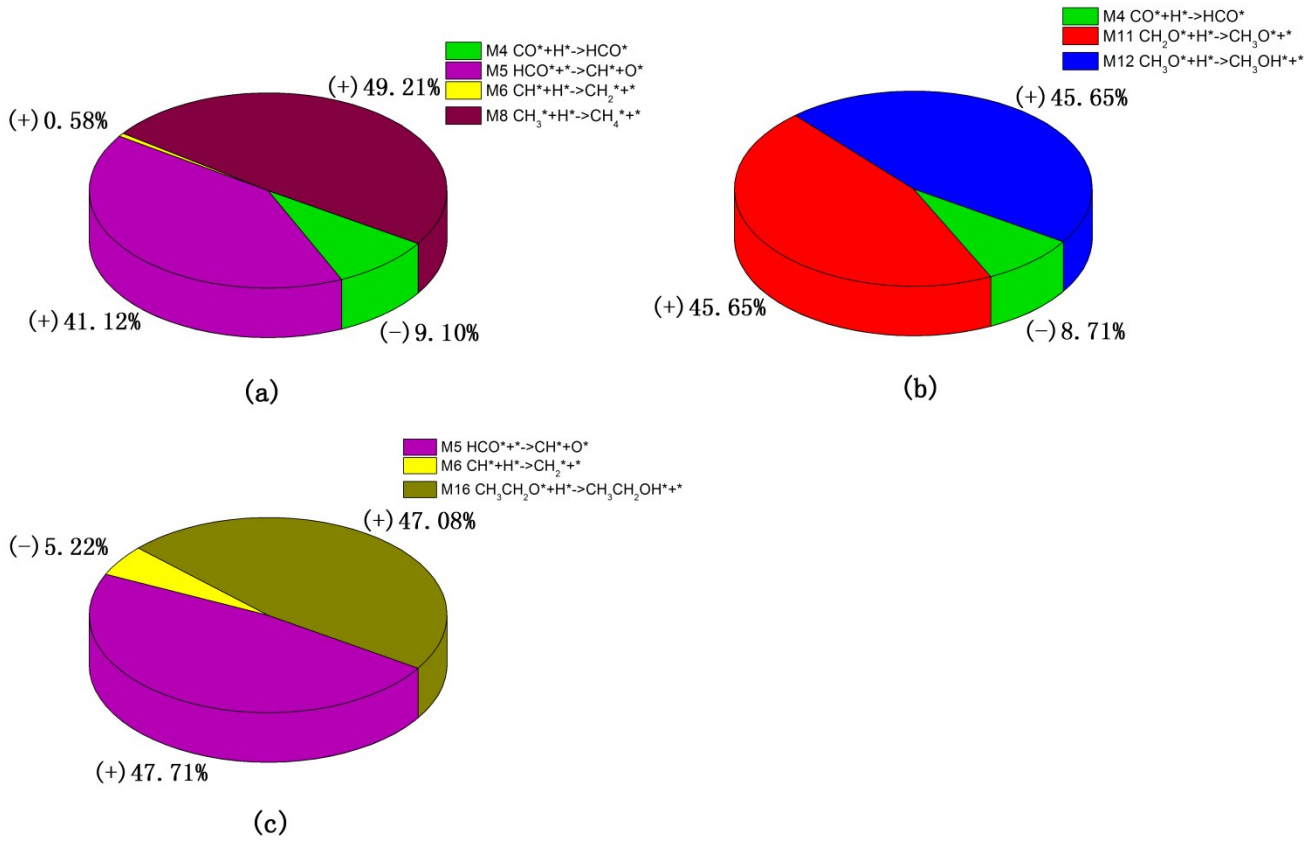

Figure S8. The DRC distribution of the elementary steps toward (a) CH_4, (b) CH_3OH and (c) CH_3CH_2OH formation on the Fe_9/Fe(100) surfaces. Note: +/− in brackets refers to the positive or negative values of DRC, corresponding to promotion or inhibition effects on the rate.

Fe_9/Fe(100) For the synthesis of methane, all the elementary steps listed in Table S8 were investigated, and steps M5 and M8 were calculated to have the main impact on the DRC as shown in Figure S8. As a result, the sensitivity analysis will focus on the hydrogenation of CO, the dissociation of HCO, the hydrogenation of CH, and the hydrogenation of CH_3 in M4, M5, M6, and M8, respectively. The dissociation of HCO in M5 and the hydrogenation of CH_3 in M8 have high DRC contributions of 41.12% and 49.21%. The steps could promote the form of CH_4 with positive DRC value toward CH_4. Obviously, elementary steps M5 and M8 are proposed to be the rate-determining steps for methane formation.

For the formation of CH_3OH, CH_2O hydrogenation and CH_3O hydrogenation have positive DRC contribution towards hydrocarbon species, indicating that the step M11 and M12 will promote the formation of CH_3OH. The CH_2O hydrogenation in M11 and CH_3O hydrogenation in M12 have

the same high DRC contributions of 45.65%. Elementary steps M11 and M12 are proposed to be the rate-limiting steps for methanol formation.

The HCO dissociation in M5 and CH_3CH_2O hydrogenation in M16 have high DRC contributions of 47.71% and 47.08%. For the formation of CH_3CH_2OH, the steps M5 and M16 have positive DRC contribution, indicating that the step M16 will promote the formation of CH_3CH_2OH. M5 and M16 are proposed to be the rate-determining steps for ethanol formation

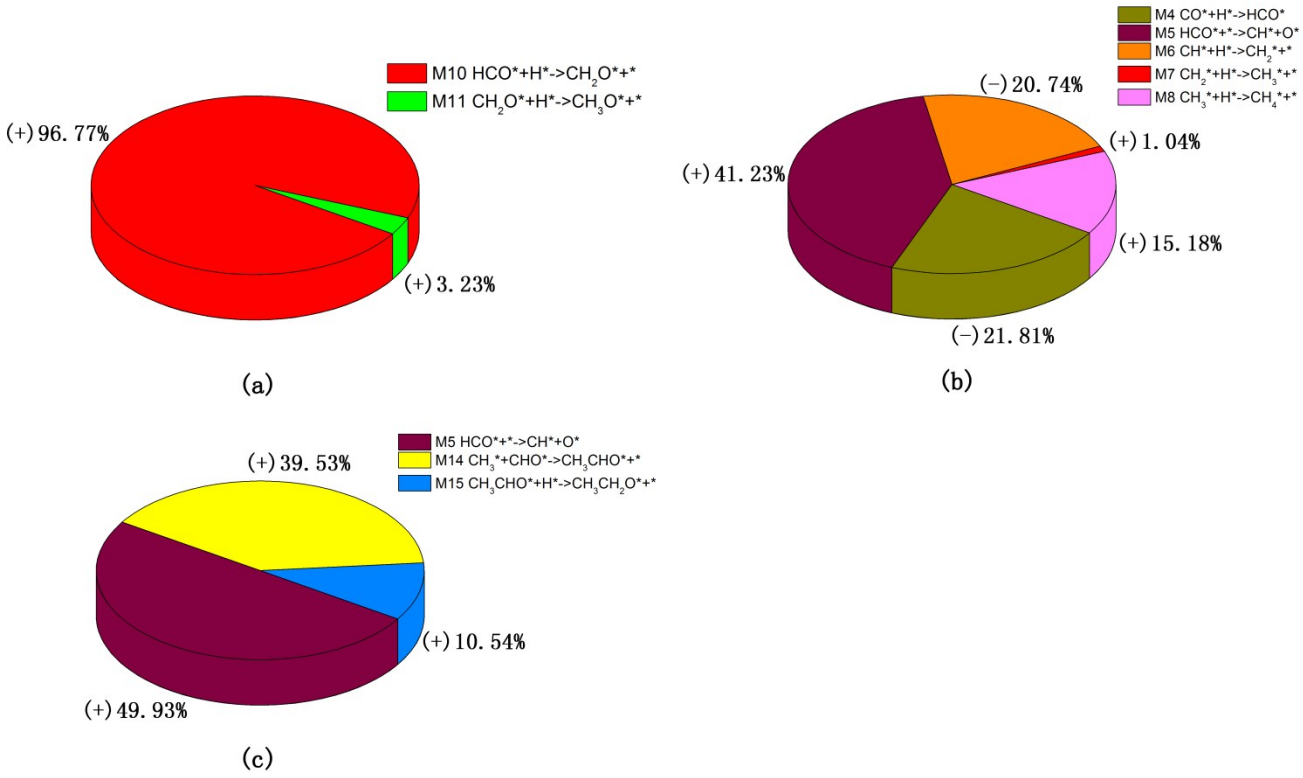

Figure S9. The DRC distribution of the elementary steps toward (a) CH_3OH, (b) CH_4 and (c) CH_3CH_2OH formation on the Cu_9/Fe(100) surfaces. Note: +/− in brackets refers to the positive or negative values of DRC, corresponding to promotion or inhibition effects on the rate.

Cu_9/Fe(100) The DRC analysis were used to reveal the rate-controlling steps to investigate the factor affecting the reactivity. In Table S9, we find that elementary reaction M10 on the Cu_9/Fe(100) site was calculated to have the main impact on the DRC shown in Figure S9. The hydrogenation of HCO in M10 has high DRC contributions of 96.77%. The step could promote the form of CH_3OH with

positive DRC value toward CH_3OH. Elementary step M10 is proposed to be the rate-determining steps for methanol formation.

For the formation of CH_4, the HCO dissociation, CH_2 hydrogenation and CH_3 hydrogenation have positive DRC contribution towards hydrocarbon species, indicating that the steps M5, M7, and M8 will promote the formation of CH_4. HCO dissociation in M5 and CH_3 hydrogenation in M8 have high DRC contributions of 41.23% and 15.18%. Obviously, elementary steps M5 and M8 are proposed to be the rate-determining steps for methane formation.

For the formation of CH_3CH_2OH, the HCO dissociation, CH_3 insertion, and CH_3CHO hydrogenation have positive DRC contribution, indicating that the steps M5, M14, and M15 will promote the formation of CH_3CH_2OH. The HCO dissociation, CH_3 insertion and CH_3CHO hydrogenation have high DRC contributions of 49.93%, 39.53%, and 10.54%. Steps M5 and M14 are proposed to be the rate-determining steps for ethanol formation.

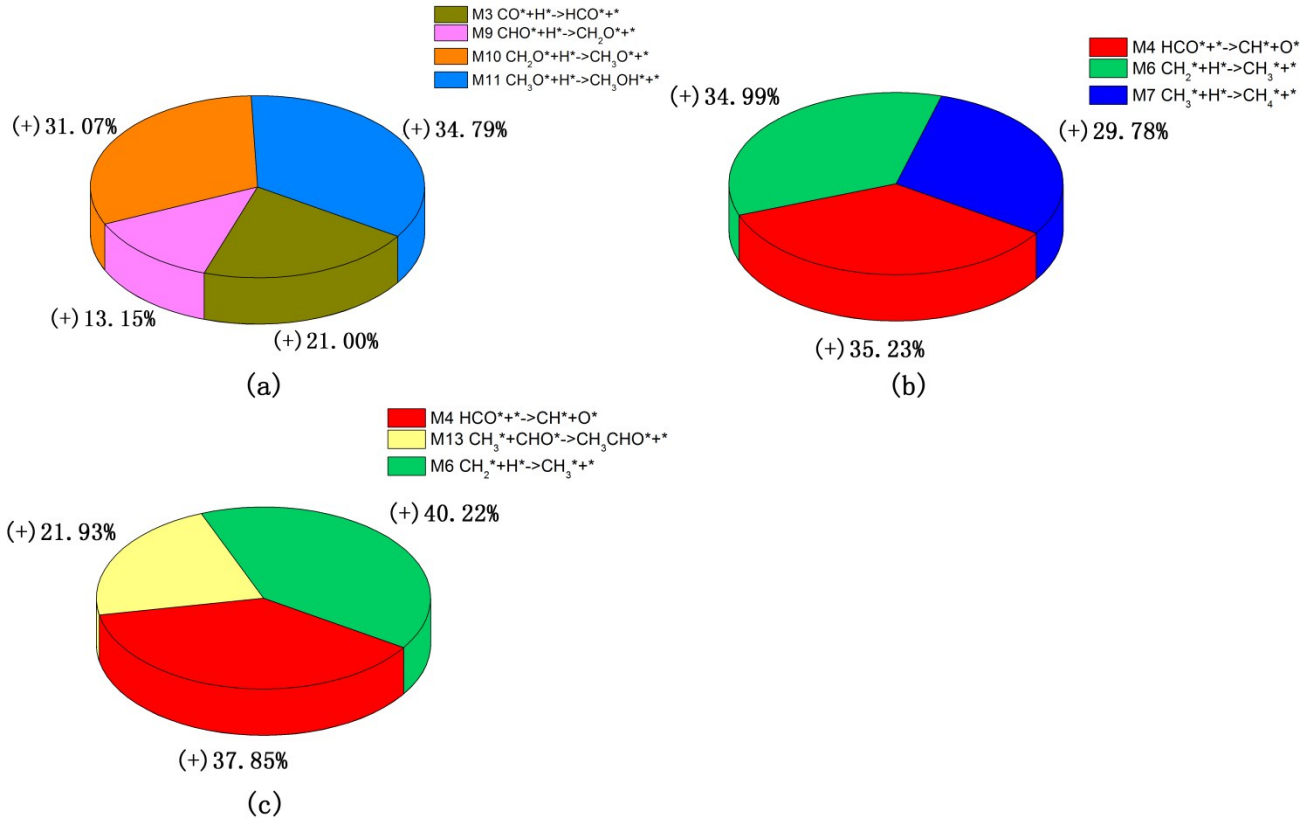

Figure S10. The DRC distribution of the elementary steps toward (a) CH_3OH, (b) CH_4 and (c) CH_3CH_2OH formation on the Pd/Fe(100) surfaces. Note: +/− in brackets refers to the positive or negative values of DRC, corresponding to promotion or inhibition effects on the rate.

Fe_3Pd_6/Fe(100) For the reaction on the Pd/Fe(100) site, as is shown in Figure 6, high reactivity into CH_3OH are gained and increase with the temperature going up. Herein, we use the DRC analysis to reveal the rate-controlling steps to get the sight of the factor affecting the reactivity. Then, we have explored all the elementary steps listed in Table S10, and find that elementary reactions M9 and M10 on the Pd/Fe(100) site were calculated to have the main impact on the DRC shown in Figure S11. As a result, the sensitivity analysis will focus on the hydrogenation of CO to HCO species, the hydrogenation of HCO to CH_2O, hydrogenation in CH_2O to CH_3O and the hydrogenation of CH_3O to CH_3OH species in M3, M9, M10, and M11, respectively. The hydrogenation of CO to HCO species in M3, the hydrogenation of HCO to CH_2O species in M9, the hydrogenation of CH_2O in M10 and the hydrogenation of CH_3O in M11 have high DRC contributions of 21.00%, 13.15%, 31.07%, and 34.79%. The steps could promote the form of CH_3OH with positive DRC value toward CH_3OH. For the formation of CH_4, the HCO dissociation, CH_2 hydrogenation and CH_3 hydrogenation have positive DRC contribution towards hydrocarbon species, indicating that the step M4, M6, and M7 will promote the formation of CH_4. The HCO dissociation in M4, CH_2 hydrogenation in M6 and CH_3 hydrogenation in M7 have high DRC contributions of 35.23%, 34.99%, and 29.78%. For the formation of CH_3CH_2OH, the HCO dissociation, CH_2 hydrogenation and CH_3 insertion have positive DRC contribution towards hydrocarbon species, indicating that the step M4, M6, and M13 will promote the formation of CH_3CH_2OH. The HCO dissociation in M4, CH_2 hydrogenation in M6 and CH_3 insertion in M13 have high DRC contributions of 37.85%, 40.22%, and 21.93%.

Table S1. Surface energies (j/m-^{2}) of iron surfaces for comparison

	Fe(100)	Fe(110)	Fe(111)	Fe(200)	Fe(210)	Fe(211)	Fe(310)
Surface energy (j/m-^{2})	2.46	2.41	2.65	2.45	2.55	2.52	2.50

Table S2. Adsorption Energies and Geometric Parameters for Various Pertinent Species in the Ethanol Synthesis Reaction on Fe_9/Fe(100)

species on Fe_9/Fe(100)	adsorption configuration	E_{ads} (eV)	D_{Fe-O} (Å)	D_{Fe-C} (Å)
CH_3CH_2OH	bridge through O	-0.27(-0.45)	2.41	-
CH_3CH_2O	bridge through O	-3.09	2.01	-
CH_3CHOH	top through O and top through C^{α}	-1.59	2.17	2.04
CH_3CHO	bridge through O and top through C^{α}	-0.85	2.01	2.11
CH_3CO	bridge through O and bridge through C^{α}	-2.68	2.00	2.02
CH_2CHO	bridge through O and bridge through C^{β}	-3.12	2.01	2.13
CH_2CO	bridge through O and bridge through C^{α}	-1.98	2.01	1.97
CHCHO	bridge through O and bridge through C^{β}	-5.17	2.07	2.08
CHCO	bridge through O and bridge through C^{β}	-3.70	2.05	1.98
CHOH	bridge through C and top through O	-3.87	2.16	2.17

CH_3OH	bridge through O	-0.20(-0.46)	2.40	-
CH_3O	bridge through O	-3.12	2.00	-
CH_2O	bridge through C and bridge through O	-1.67	2.02	2.15
COH	4-fold hollow through C	-4.55	-	2.03
HCO	bridge through C and bridge through O	-3.04	2.00	1.99
CO	4-fold hollow through C and bridge through O	-2.07(-1.47)	2.14	1.96
CH_4	4-fold hollow	0.10(-0.15)	-	3.99
CH_3	top through C	-1.88	-	2.07
CH_2	4-fold hollow through C	-4.66	-	2.14
CH	4-fold hollow through C	-7.37	-	2.04
H_2O	bridge through O	-0.21(-0.32)	2.39	
H_2	top through H	-0.19(-0.01)	1.72	
O	4-fold hollow through C	-7.04	2.06	-
H	4-fold hollow through H	-2.66	-	2.03
C	4-fold hollow through C	-8.48	-	1.96

Note: Entries in parentheses are the energies after vDW-DF correction

Table S3. Adsorption Energies and Geometric Parameters for Various Pertinent Species in the Ethanol Synthesis Reaction on $Cu_9/Fe(100)$

species on $Cu_9/Fe(100)$	adsorption configuration	E_{ads} (eV)	d_{Fe-O} (Å)	d_{Fe-C} (Å)
CH_3CH_2OH	top through O	-0.30(-0.58)	2.27	-
CH_3CH_2O	bridge through O	-2.43	2.00	-
CH_3CHOH	bridge through O and bridge through C^{α}	-1.02	2.22	2.06
CH_3CHO	bridge through O and bridge through C^{α}	-0.07	2.06	2.22
CH_3CO	bridge through O and bridge through C^{α}	-1.35	2.15	2.08
CH_2CHO	bridge through O and bridge through C^{β}	-2.02	2.09	2.24
CH_2CO	bridge through O and bridge through C^{α}	-0.83	2.04	1.98
CHCHO	bridge through O and bridge through C^{β}	-4.13	2.07	2.02
CHCO	bridge through C^{α} and bridge through C^{β}	-2.34	-	2.17/2.01

CH_2OH	bridge through C and bridge through O		-1.25	2.39	2.14
CHOH	bridge through C and bridge through O		-2.81	2.56	2.23
CH_3OH	bridge through O	-	-0.20(-0.53)	2.31	-
CH_3O	bridge through O		-2.48	1.98	-
CH_2O	bridge through C and bridge through O		-0.45	2.04	2.16
COH	4-fold hollow through C		-3.17	-	2.08/2.12
HCO	bridge through C and bridge through O		-1.52	2.05	2.09
CO	4-fold hollow through C and bridge through O		-0.92(-0.54)	-	2.23
CH_4	4-fold hollow through C		-0.01(-0.32)	-	3.52
CH_3	bridge through C		-1.54	-	2.12
CH_2	4-fold hollow through C	-	-3.57	-	2.17
CH	4-fold hollow through C		-6.15	-	2.05
H_2O	bridge through O		-0.09(-0.27)	2.39	
H_2	top through H		0.03(-0.39)	2.84	
O	4-fold hollow through C		-5.79	2.10	-
H	4-fold hollow through H		-2.41	-	2.00
C	4-fold hollow through C		-6.81	-	1.99

Note: Entries in parentheses are the energies after vDW-DF correction

Table S4. Adsorption Energies and Geometric Parameters for Various Pertinent Species in the Ethanol Synthesis Reaction on Fe_3Pd_6/Fe(100)

species on Cu/Fe(100)	adsorption configuration	E_{ads} (eV)	$d_{Fe\text{-}O/Pd\text{-}O}$ (Å)	$D_{Fe\text{-}C/Pd\text{-}C}$ (Å)
CH_3CH_2OH	top through O	-0.47	2.17/-	-
CH_3CH_2O	bridge through O	-2.93	1.96/-	-
CH_3CHOH	bridge through O and top through C^{α}	-1.32	2.26	2.70/2.14

CH_3CHO	bridge through O and top through C^{α}		-0.69	2.03	2.65/2.16
CH_3CO	bridge through O and bridge through C^{α}		-2.21	2.03/-	2.00/2.16
CH_2CHO	top through O and top through C^{β}		-5.15	1.94/-	2.13/2.32
CH_2CO	bridge through O and bridge through C^{α}		1.52	2.01/-	2.00/2.25
CHCHO	bridge through O and bridge through C^{β}		-4.51	2.04/-	2.01/2.21
CHCO	bridge through O and bridge through C^{β}		-2.89	2.08/-	1.98/2.26
CH_2OH	top through C and top through O		-1.49	2.18/-	2.11/2.34
CHOH	bridge through C and top through O		-3.53	2.25/-	1.92/2.11
CH_3OH	bridge through O	-	-0.36	-	2.31/-
CH_3O	bridge through O		-2.91	-	1.96/-
CH_2O	bridge through C and bridge through O		-1.06	2.00/-	2.29/2.19
COH	4-fold hollow through C		-3.87	-	2.06/2.18
HCO	bridge through C and bridge through O		-2.05	2.02/-	1.96/2.16
CO	4-fold hollow through C and bridge through O		-1.34	2.13/-	1.93/2.10
CH_4	4-fold hollow		0.08	-	3.64/-
CH_3	bridge through C		-1.81	-	2.15/-
CH_2	4-fold hollow through C	-	-3.90	-	2.03/2.31
CH	4-fold hollow through C		-6.70	-	1.98/2.17
O	4-fold hollow through C		-6.28	1.90/2.48	-
H	4-fold hollow through H		-2.59	-	1.88/2.06
C	4-fold hollow through C		-7.74	-	1.92/2.08

Table S5. Calculated reaction energies (ΔE), energy barriers (E_a), and the forming bond lengths of TSs on Fe_9/Fe(100) surface in this work

Reaction	ΔE/ eV	E_a/ eV	d/ Å
M1 CO(g)+*→CO*	-2.07	-	-
M2 H_2(g)+*→H_2*	-0.01	-	-
M3 CO*+ *→C*+O*	-0.89	1.10(1.18)	1.94
M4 H_2* → H* + H*	-0.62	0.02(0.02)	0.98
M5 CO*+ H*→HCO*+*	0.53	0.82(0.82)	1.48
M6 HCO*+ *→CH*+O*	-1.41	0.50(0.56)	1.93
M7 HCO*+ H*→CH_2O*+*	-0.10	0.90(0.90)	1.68
M8 HCO*+ H*→CHOH*+*	1.12	1.49(1.43)	1.33
M9 CH_2O*+ *→CH_2*+O*	-0.92	0.85(0.91)	2.08
M10 CH_2O*+ H*→CH_3O*+*	-0.52	0.81(0.85)	1.82
M11 CH_3O*+ *→CH_3*+O*	-0.93	1.67(1.70)	2.23
M12 CH_3O*+H *→CH_3OH*+*	0.52	1.50(1.47)	1.28
M13 CH_3OH*→CH_3OH(g)+*	0.20	-	-
M14 CH*+ CO*→CHCO*+*	1.24	1.83(1.79)	1.46
M15 CH*+ HCO*→CHCHO*+*	0.17	1.79(1.79)	1.89
M16 CH_2*+ CO*→CH_2CO*+*	0.18	1.85(1.81)	2.12
M17 CH_2*+ HCO*→CH_2CHO*+*	-0.28	1.78(1.75)	2.12
M18 CH_3*+ CO*→CH_3CO*+*	0.16	2.16(2.19)	2.05
M19 CH_3*+ HCO*→CH_3CHO*+*	0.23	1.76(1.76)	2.11
M20 CH*+H *→CH_2*+*	0.51	0.75(0.79)	1.54
M21 CH_2*+H *→CH_3*+*	-0.55	0.76(0.76)	1.68
M22 CH_3*+H *→CH_4*+*	-0.45	0.80(0.80)	1.90
M23 CH_4*→CH_4(g)+*	-0.10	-	-
M24 CH_3CHO*+H*→CH_3CHOH*+*	0.86	1.49(1.43)	1.34
M25 CH_3CHO*+H*→CH_3CH_2O*+*	-0.11	0.82(0.82)	1.91
M26 CH_3CH_2O*+H*→CH_3CH_2OH*+*	0.83	1.55(1.55)	1.27

M27$CH_3CH_2OH^* \rightarrow CH_3CH_2OH(g)+*$	0.27	-	-
M28 $O^* + H^* \rightarrow OH^* + *$	0.10	1.30(1.41)	1.32
M29 $OH^* + * \rightarrow H_2O^* + *$	0.42	1.20(1.25)	1.25
M30$H_2O^* \rightarrow H_2O(g)+*$	0.32	-	-

Note: Entries in parentheses are the energies before ZPE

Table S6. Calculated reaction energies (ΔE), energy barriers (E_a), and the forming bond lengths of TSs on Cu_9/Fe(100) surface in this work

Reaction	ΔE/ eV	E_a/ eV	d/ Å
M1$CO(g)+* \rightarrow CO^*$	-0.92	-	-
M2$H_2(g)+* \rightarrow H_2^*$	-0.25	-	-
M3 $CO^*+ * \rightarrow C^*+O^*$	0.57	2.32(2.38)	1.97
M4 $H_2^* + * \rightarrow H^* + H^*$	-0.31	0.30(0.30)	1.26
M5 $CO^*+ H^* \rightarrow HCO^*+*$	0.75	1.07(1.07)	1.55
M6 $HCO^*+ * \rightarrow CH^*+O^*$	-0.57	0.99(1.02)	1.93
M7 $HCO^*+ H^* \rightarrow CH_2O^*+*$	-0.45	0.59(0.59)	1.93
M8 $HCO^*+ H^* \rightarrow CHOH^*+*$	0.47	1.06(1.09)	1.41
M9 $CH_2O^*+ * \rightarrow CH_2^*+O^*$	0.11	1.83(1.89)	2.39
M10 $CH_2O^*+ H^* \rightarrow CH_3O^*+*$	-0.69	0.50(0.50)	2.51
M11 $CH_2O^*+ H^* \rightarrow CH_2OH^*+*$	0.24	2.00(1.89)	1.44
M12 $CH_3O^*+ * \rightarrow CH_3^*+O^*$	-0.02	1.56(1.63)	2.23
M13 $CH_3O^*+H * \rightarrow CH_3OH^*+*$	0.03	0.74(0.74)	1.43
M14 $CH_3OH^* \rightarrow CH_3OH(g)+*$	0.20	-	-
M15 $CH^*+ CO^* \rightarrow CHCO^*+*$	0.33	1.07(1.07)	1.94
M16 $CH^*+ HCO^* \rightarrow CHCHO^*+*$	-0.90	0.79(0.79)	2.09
M17 $CH_2^*+ CO^* \rightarrow CH_2CO^*+*$	-0.70	1.12(1.12)	2.19
M18 $CH_2^*+ HCO^* \rightarrow CH_2CHO^*+*$	-0.82	0.93(0.98)	2.32
M19 $CH_3^*+ CO^* \rightarrow CH_3CO^*+*$	-0.01	1.68(1.59)	2.08
M20 $CH_3^*+ HCO^* \rightarrow CH_3CHO^*+*$	-1.05	0.77(0.77)	2.69
M21 $CH^*+H * \rightarrow CH_2^*+*$	0.25	0.89(0.92)	1.78

M22 CH_2*+H *→CH_3*+*	-0.53	0.91(0.94)	1.85
M23 CH_3*+H *→CH_4*+*	-0.89	1.20(1.20)	2.42
M24 CH_4*→CH_4(g)+*	0.01	-	-
M25 CH_3CHO*+H*→CH_3CHOH*+*	0.29	1.53(1.49)	1.41
M26 CH_3CHO*+H*→CH_3CH_2O*+*	-0.62	0.67(0.63)	2.06
M27 CH_3CH_2O*+H*→CH_3CH_2OH*+*	-0.07	1.11(1.11)	1.63
M28 CH_3CH_2OH*→CH_3CH_2OH(g)+*	0.30	-	-
M29 O* + H* → OH* + *	0.08	1.20(1.29)	1.48
M30 OH* + H* → H_2O* + *	-0.03	0.61(0.67)	1.43
M31 H_2O*→H_2O(g)+*	0.39	-	-

Note: Entries in parentheses are the energies before ZPE

Table S7. Calculated reaction energies (ΔE), energy barriers (E_a), and the forming bond lengths of TSs on Fe_3Pd_6/Fe(100) surface in this work

Reaction	ΔE/ eV	E_a/ eV	d/ Å
M1 CO(g)+ * →CO*	-1.34	-	-
M2 H_2(g)+ * →H_2*	-0.04	-	-
M3 CO*+ *→C*+O*	0.28	1.19	1.93
M4 H_2* + * →H*+H*	-0.59	0.15	1.84
M5 CO*+ H*→HCO*+*	0.19	0.77	1.50
M6 HCO*+ *→CH*+O*	-0.15	0.93	1.90
M7 HCO*+ H*→CH_2O*+*	-0.01	0.70	1.69
M8 HCO*+ H*→CHOH*+*	0.80	1.44	1.26
M9 CH_2O*+ *→CH_2*+O*	0.22	1.12	2.08
M10 CH_2O*+ H*→CH_3O*+*	-0.53	0.70	2.08
M11 CH_2O*+ H*→CH_2OH*+*	0.53	2.01	1.28
M12 CH_3O*+ *→CH_3*+O*	0.10	1.70	2.14
M13 CH_3O*+H *→CH_3OH*+*	0.17	0.64	1.36
M14 CH_3OH*→CH_3OH(g)+*	0.36	-	-
M15 CH*+ CO*→CHCO*+*	0.59	0.75	1.38

M16 CH*+ HCO*→CHCHO*+*	-1.18	1.12	1.98
M17 CH_2*+ CO*→CH_2CO*+*	-0.47	0.33	1.51
M18 CH_2*+ HCO*→CH_2CHO*+*	-1.68	0.12	2.25
M19 CH_3*+ CO*→CH_3CO*+*	-0.24	1.27	2.04
M20 CH_3*+ HCO*→CH_3CHO*+*	-0.74	0.82	1.95
M21 CH*+H *→CH_2*+*	0.50	0.76	1.53
M22 CH_2*+H *→CH_3*+*	-0.42	0.85	1.68
M23 CH_3*+H *→CH_4*+*	-0.35	0.79	1.57
M24 CH_4*→CH_4(g)+*	-0.08	-	-
M25 CH_3CHO*+H*→CH_3CHOH*+*	0.58	1.87	1.33
M26 CH_3CHO*+H*→CH_3CH_2O*+*	-0.53	0.47	2.86
M27 CH_3CH_2O*+H*→CH_3CH_2OH*+*	0.25	0.83	1.37
M28 CH_3CH_2OH*→CH_3CH_2OH(g)+*	0.47	-	-
M29 O* + H* → OH* + *	-0.13	1.38	1.44
M30 OH* + H* → H_2O* + *	0.19	1.03	1.39
M31 H_2O*→H_2O(g)+*	0.36	-	-

Table S8. The d-band center and d-band width of Cu/Fe surfaces (unit: eV)

	Fe_3Cu_6/Fe(100)	Fe_9/Fe(100)	Cu_9/Fe(100)	Fe_3Pd_6/Fe(100)
d-band center (eV)	-1.06	-0.87	-2.11	-1.12

Table S9. The ICOHP value for the interaction between C and Fe on Cu/Fe and Pd/Fe surfaces.

	Fe_9/Fe(100)	Fe_3Cu_6/Fe(100)	Fe_3Pd_6/Fe(100)	Cu_9/Fe(100)
ICOHP	-1.04	-0.42	-0.36	-0.11

Table S10. Elementary Reaction Steps and Kinetic Parameters for Ethanol Reaction on Fe_3Cu_6/Fe(100) in This Work at 483 K

reaction	E_a (eV)	A	E_a^{-1} (eV)	A^{-1}
M1 CO(g) + * → CO*	0.0	1.6×10^{3}	33.2	5.5×10^{17}
M2 H_2(g) + * → H_2*	0.0	6.0×10^{3}	16.1	6.2×10^{14}
M3 H_2* + * → H* + H*	4.6	4.3×10^{12}	14.7	5.5×10^{13}
M4 CO* + H* → HCO* + *	18.3	1.9×10^{13}	3.2	1.8×10^{13}
M5 HCO* + * → CH* + O*	12.8	9.3×10^{12}	32.6	1.5×10^{13}
M6 CH* + H* → CH_2* + *	17.1	1.5×10^{13}	5.6	1.5×10^{13}
M7 CH_2* + H* → CH_3* + *	18.4	3.2×10^{13}	20.7	9.0×10^{12}
M8 CH_3* + H* → CH_4* + *	18.0	3.3×10^{13}	25.6	3.0×10^{12}
M9 CH_4* → CH_4(g) + *	2.0	9.6×10^{15}	0.0	2.1×10^{3}
M10 HCO* + H* → CH_2O* + *	20.0	2.7×10^{13}	20.5	3.0×10^{13}
M11 CH_2O* + H* → CH_3O* + *	18.3	3.5×10^{13}	26.8	1.6×10^{13}
M12 CH_3O* + H* → CH_3OH* + *	26.3	3.5×10^{13}	9.8	1.3×10^{13}
M13 CH_3OH* → CH_3OH(g) + *	6.0	2.8×10^{17}	0.0	1.5×10^{3}
M14 CH_3* + CHO*→ CH_3CHO* + *	21.8	9.9×10^{12}	32.1	7.5×10^{12}
M15 CH_3CHO* + H* → CH_3CHOH* + *	8.0	2.6×10^{13}	2.4	2.7×10^{13}
M16 CH_3CHOH* + H* → CH_3CH_2OH* + *	17.2	1.3×10^{13}	24.0	6.6×10^{12}
M17 CH_3CH_2OH* → CH_3CH_2OH(g) + *	10.9	2.1×10^{18}	0.0	1.3×10^{3}
M18 O* + H* → OH* + *	30.7	3.0×10^{13}	37.2	3.2×10^{13}
M19 OH* + H* → H_2O* + *	26.8	2.7×10^{13}	36.3	1.1×10^{13}
M20 H_2O* → H_2O(g) + *	7.6	3.7×10^{16}	0.0	2.0×10^{3}

Table S11. Elementary Reaction Steps and Kinetic Parameters for Ethanol Reaction on Fe_9/Fe(100) in This Work at 483 K

reaction	E_a (eV)	A	E_a^{-1} (eV)	A^{-1}
M1 CO(g) + * → CO*	0.0	5.3×10^{3}	30.8	7.1×10^{17}
M2 H_2(g) + * → H_2*	0.0	6.5×10^{3}	0.1	7.9×10^{14}
M3 H_2* + * → H* + H*	0.0	1.1×10^{13}	14.7	7.7×10^{12}
M4 CO* + H* → HCO* + *	17.8	1.1×10^{13}	9.8	1.7×10^{13}
M5 HCO* + * → CH* + O*	23.7	1.3×10^{13}	25.3	1.9×10^{13}
M6 CH* + H* → CH_2* + *	17.5	1.3×10^{13}	4.1	8.6×10^{12}

M7 CH_2* + H* → CH_3* + *	14.9	1.1×10^{13}	20.7	7.6×10^{12}
M8 CH_3* + H* → CH_4* + *	18.3	2.0×10^{13}	23.3	2.8×10^{12}
M9 CH_4* → CH_4(g) + *	1.9	1.3×10^{16}	0.0	2.3×10^{3}
M10 HCO* + H* → CH_2O* + *	13.4	1.4×10^{13}	10.5	1.3×10^{13}
M11 CH_2O* + H* → CH_3O* + *	13.5	2.1×10^{13}	22.4	9.1×10^{12}
M12 CH_3O* + H* → CH_3OH* + *	14.8	1.0×10^{13}	5.1	7.1×10^{12}
M13 CH_3OH* → CH_3OH(g) + *	8.2	3.6×10^{17}	0.0	1.6×10^{3}
M14 CH_3* + CHO*→ CH_3CHO* + *	18.9	3.0×10^{13}	34.8	2.7×10^{13}
M15 CH_3CHO* + H* → CH_3CH_2O* + *	10.7	3.1×10^{13}	18.8	2.2×10^{13}
M16 CH_3CH_2O* + H* → CH_3CH_2OH* + *	19.3	2.0×10^{13}	8.3	6.9×10^{12}
M17 CH_3CH_2OH* → CH_3CH_2OH(g) + *	11.0	2.0×10^{18}	0.0	1.3×10^{3}
M18 O* + H* → OH* + *	30.0	2.2×10^{13}	37.2	1.4×10^{13}
M19 OH* + * → H_2O*	27.7	1.5×10^{13}	36.3	4.0×10^{13}
M20 H_2O + * → H_2O(g)	7.65	9.8×10^{17}	0.0	9.9×10^{8}

Table S12. Elementary Reaction Steps and Kinetic Parameters for Ethanol Reaction on Cu_9/Fe(100) in This Work at 483 K

reaction	E_a (eV)	A	E_a^{-1} (eV)	A^{-1}
M1 CO(g) + * → CO*	0.0	5.3×10^{3}	21.2	8.1×10^{17}
M2 H_2(g) + * → H_2*	0.0	6.5×10^{3}	16.1	7.9×10^{14}
M3 H_2* → H* + H*	6.9	1.1×10^{12}	14.1	9.1×10^{12}
M4 CO* + H* → HCO* + *	24.6	1.8×10^{13}	4.2	2.1×10^{13}
M5 HCO* + * → CH* + O*	22.8	1.2×10^{13}	37.5	1.8×10^{13}
M6 CH* + H* → CH_2* + *	20.5	1.5×10^{13}	12.8	1.2×10^{13}
M7 CH_2* + H* → CH_3* + *	21.1	3.1×10^{13}	53.4	1.1×10^{12}
M8 CH_3* + H* → CH_4* + *	15.0	1.6×10^{13}	8.6	5.0×10^{12}
M9 CH_4* → CH_4(g) + *	1.8	4.1×10^{17}	0.0	1.6×10^{3}
M10 HCO* + H* → CH_2O* + *	17.8	2.3×10^{13}	11.5	3.8×10^{13}
M11 CH_2O* + H* → CH_3O* + *	15.6	1.2×10^{13}	24.1	3.4×10^{13}
M12 CH_3O* + H* → CH_3OH* + *	16.8	2.7×10^{13}	7.1	6.8×10^{12}
M13 CH_3OH* → CH_3OH(g) + *	4.6	2.1×10^{17}	0.0	1.3×10^{3}
M14 CH_3* + CHO*→ CH_3CHO* + *	27.7	5.0×10^{13}	30.0	7.4×10^{13}
M15 CH_3CHO* + H* → CH_3CH_2O* + *	11.4	3.4×10^{13}	20.1	2.7×10^{13}
M16 CH_3CH_2O* + H* → CH_3CH_2OH* + *	17.3	2.3×10^{13}	8.9	7.2×10^{12}

M17 $CH_3CH_2OH^* \rightarrow CH_3CH_2OH(g) + *$	6.8	2.0×10^{18}	0.0	1.3×10^{3}
M18 $O^* + H^* \rightarrow OH^* + *$	27.7	1.9×10^{13}	28.8	5.6×10^{13}
M19 $OH^* + H^* \rightarrow H_2O^* + *$	14.0	7.2×10^{12}	12.7	6.1×10^{8}
M20 $H_2O^* \rightarrow H_2O(g) + *$	8.99	9.8×10^{8}	0.0	9.9×10^{8}

Table S13. Elementary Reaction Steps and Kinetic Parameters for Ethanol Reaction on Fe_3Pd_6/Fe(100) in This Work at 483 K

reaction	E_a (eV)	A	E_a^{-1} (eV)	A^{-1}
M1 $CO(g) + * \rightarrow CO^*$	0.0	5.3×10^{3}	30.8	7.1×10^{17}
M2 $H_2(g) + * \rightarrow H_2^*$	0.0	6.5×10^{3}	15.0	7.9×10^{14}
M3 $H_2^* \rightarrow H^* + H^*$	6.9	1.1×10^{12}	14.1	9.1×10^{12}
M4 $CO^* + H^* \rightarrow HCO^* + *$	17.8	1.1×10^{13}	9.8	1.7×10^{13}
M5 $HCO^* + * \rightarrow CH^* + O^*$	23.7	1.3×10^{13}	25.3	1.9×10^{13}
M6 $CH^* + H^* \rightarrow CH_2^* + *$	17.5	1.3×10^{13}	4.1	8.6×10^{12}
M7 $CH_2^* + H^* \rightarrow CH_3^* + *$	14.9	1.1×10^{13}	20.7	7.6×10^{12}
M8 $CH_3^* + H^* \rightarrow CH_4^* + *$	18.3	2.0×10^{13}	23.3	2.8×10^{12}
M9 $CH_4^* \rightarrow CH_4(g) + *$	1.9	1.3×10^{16}	0.0	2.3×10^{3}
M10 $HCO^* + H^* \rightarrow CH_2O^* + *$	13.4	1.4×10^{13}	10.5	1.3×10^{13}
M11 $CH_2O^* + H^* \rightarrow CH_3O^* + *$	13.5	2.1×10^{13}	22.4	9.1×10^{12}
M12 $CH_3O^* + H^* \rightarrow CH_3OH^* + *$	14.8	1.0×10^{13}	5.1	7.1×10^{12}
M13 $CH_3OH^* \rightarrow CH_3OH(g) + *$	8.2	3.6×10^{17}	0.0	1.6×10^{3}
M14 $CH_3^* + CHO^* \rightarrow CH_3CHO^* + *$	18.9	3.0×10^{13}	34.8	2.7×10^{13}
M15 $CH_3CHO^* + H^* \rightarrow CH_3CH_2O^* + *$	10.7	3.1×10^{13}	18.8	2.2×10^{13}
M16 $CH_3CH_2O^* + H^* \rightarrow CH_3CH_2OH^* + *$	19.3	2.0×10^{13}	8.3	6.9×10^{12}
M17 $CH_3CH_2OH^* \rightarrow CH_3CH_2OH(g) + *$	11.0	2.0×10^{18}	0.0	1.3×10^{3}
M18 $O^* + H^* \rightarrow OH^* + *$	31.8	1.9×10^{13}	32.8	5.6×10^{13}
M19 $OH^* + H^* \rightarrow H_2O^* + *$	23.8	7.2×10^{12}	22.7	6.1×10^{8}
M20 $H_2O^* \rightarrow H_2O(g) + *$	8.99	9.8×10^{8}	0.0	9.9×10^{8}